

# DeepLuAd: Semantic-guided virtual histopathology of lung adenocarcinoma via stimulated Raman scattering

Liyang Ma<sup>1</sup>, Yuheng Guo<sup>1</sup>, Yongjun Cai<sup>2</sup>, Min Du<sup>2</sup>, Lin Qi<sup>2\*</sup>, Minbiao Ji<sup>1\*</sup>

1.State Key Laboratory of Surface Physics and Department of Physics, Human Phenome Institute, Academy for Engineering and Technology, Fudan University, 200433 Shanghai, China.

2.Huadong Hospital Affiliated to Fudan University, 200040 Shanghai, China.

## Abstract

Lung adenocarcinoma - the most common type of lung cancer, demands accurate diagnostic grading to guide effective clinical management. Current gold-standard Hematoxylin and Eosin (H&E) staining provides morphological contrast but lacks biochemical specificity, limiting quantitative analysis of tissue subtypes within the heterogeneous lung cancer microenvironments. We developed DeepLuAd, an AI-powered platform integrating label-free stimulated Raman scattering (SRS) microscopy with semantic-guided deep learning, enabling automated tumor grading, cellular-level morpho-chemical quantification, and unsupervised virtual H&E staining. The platform achieved a mean intersection-over-union (mIOU) of 80.43% across tissue subtypes, and a grading concordance rate of 76.2% with clinical diagnoses (16/21 cases). Moreover, it quantifies lipid-to-protein ratio heterogeneity within tumor and stromal regions, revealing biochemical signatures of disease progression. The modular and scalable DeepLuAd framework may also be broadly applicable to diverse solid tumors for AI-enhanced histopathology.

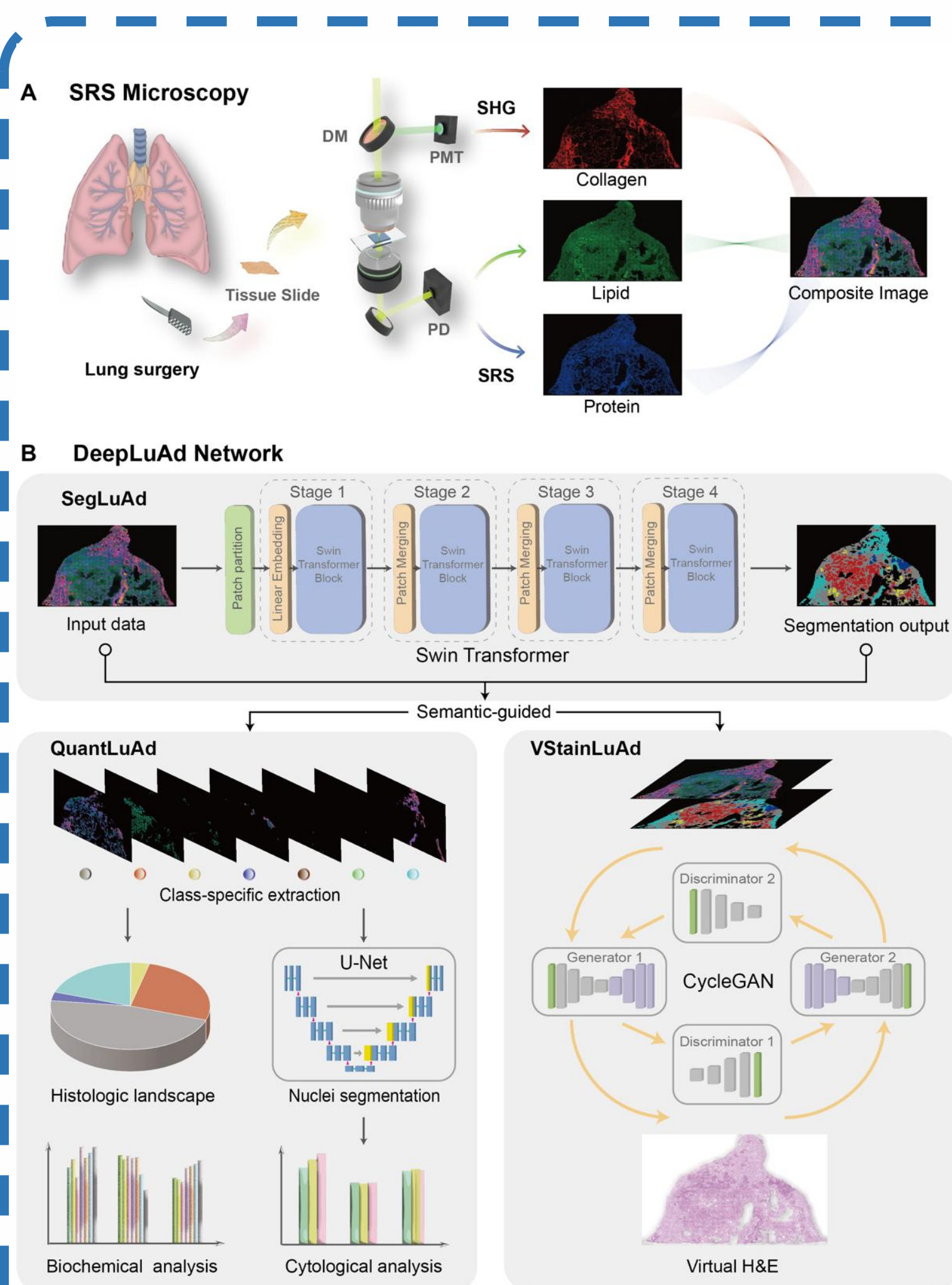


**Figure 1. Workflow of SRS imaging and deep-learning platform for virtual histopathology of lung adenocarcinoma.** (A) Label-free SRS microscopy for lung surgical tissue specimens, with dual SRS channels of lipid (green) and protein (blue), and an SHG channel of collagen fibers (red). (B) Multi-task DeepLuAd network composed of three AI modules: SegLuAd for semantic segmentation of tissue classes; QuantLuAd for quantitative biochemical and cytological feature analysis; and VStainLuAd for virtual H&E staining.

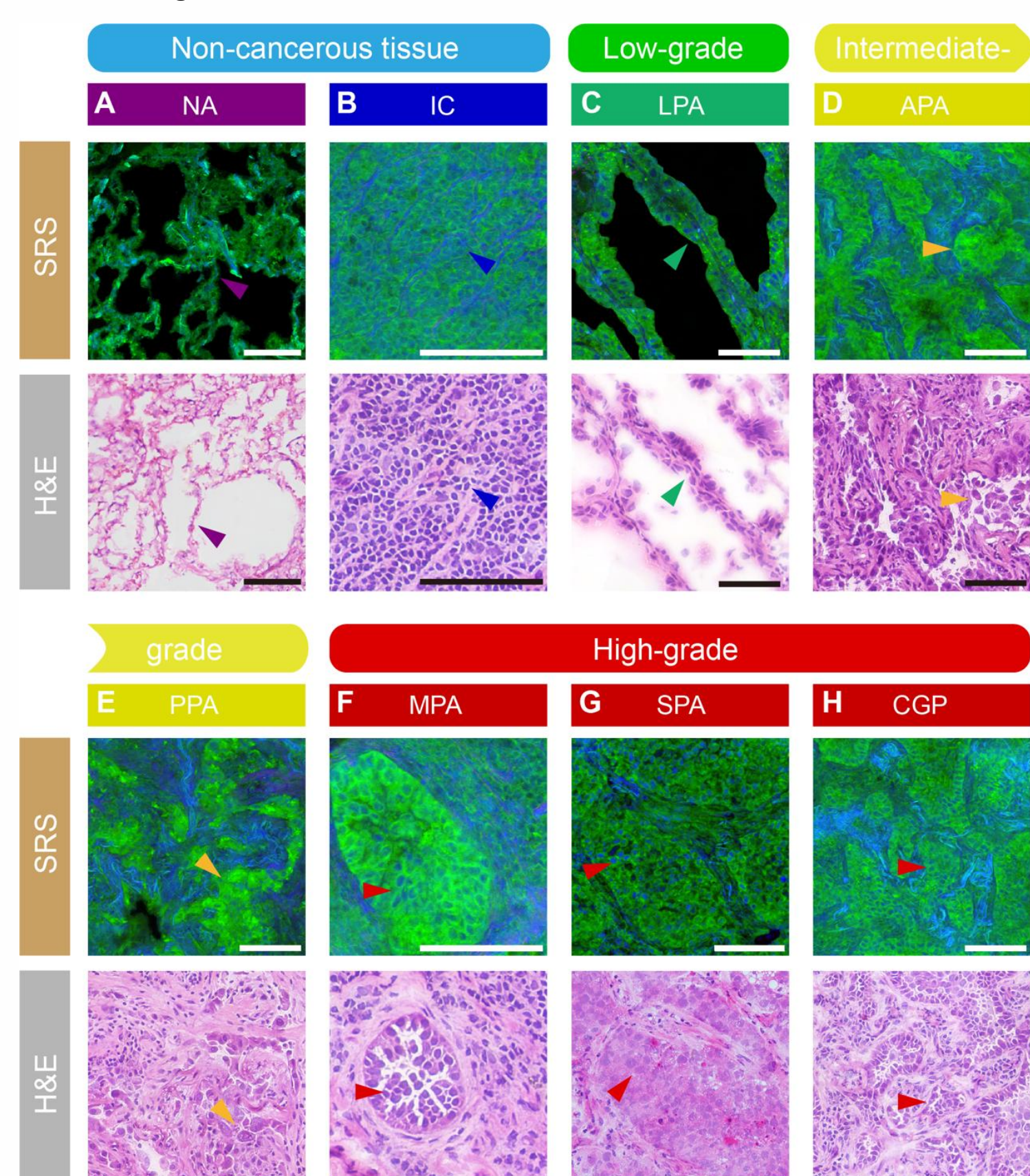


**Figure 2. Representative SRS and H&E images of adjacent sections reveal major histologic features of tissue subtypes.** Arrows indicate key diagnostic morphological cues. (A) Normal alveoli (NA). (B) Immune cells (IC). (C) Lepidic predominant adenocarcinoma (LPA). (D) Acinar predominant adenocarcinoma (APA). (E) Papillary predominant adenocarcinoma (PPA). (F) Micropapillary predominant adenocarcinoma (MPA). (G) Solid predominant adenocarcinoma (SPA). (H) Complex glandular patterns (CGP). Scale bars: 100  $\mu$ m.

## Result

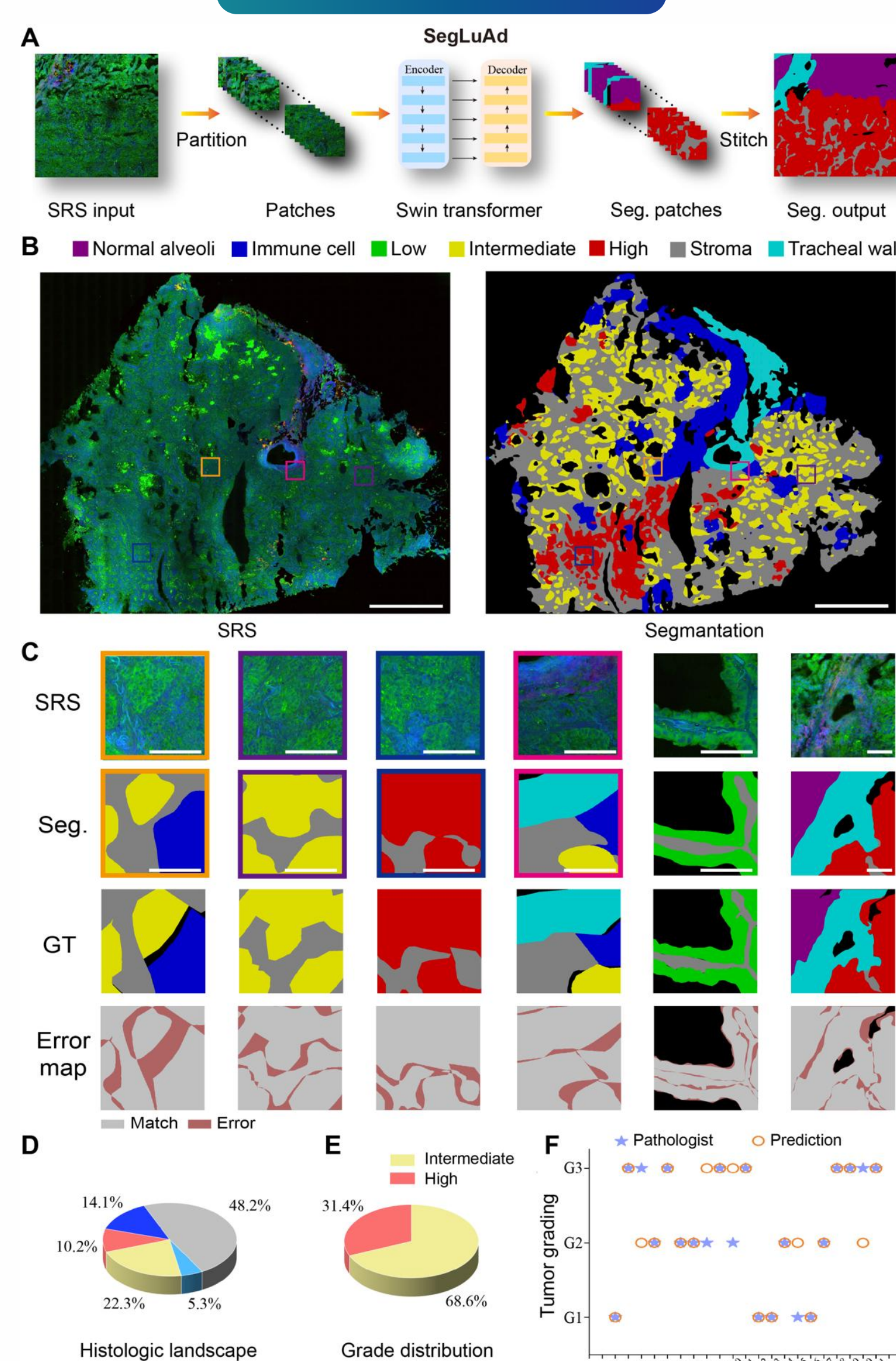


**Figure 3. SegLuAd module for histologic segmentation of seven tissue classes.** (A) Schematic workflow of SegLuAd pipeline. (B) Representative whole-slide SRS image and corresponding segmentation output. (C) Magnified images of representative regions: SRS data, segmentation results, annotated ground truth and error map. (D) Quantified area percentages of different tissue classes. (E) Tumor grade distribution derived from subtypes partition. (F) Clinical validation on an external cohort of 21 cases, showing a grading consistency rate of 76.2%. Color coding for (B-D): Low grade (green), Intermediate grade (yellow), High grade (red), Immune cells (dark blue), Normal alveoli (purple), Stroma (gray), Tracheal wall (cyan). Scale bars: 1000  $\mu$ m in (B), 100  $\mu$ m in (C).

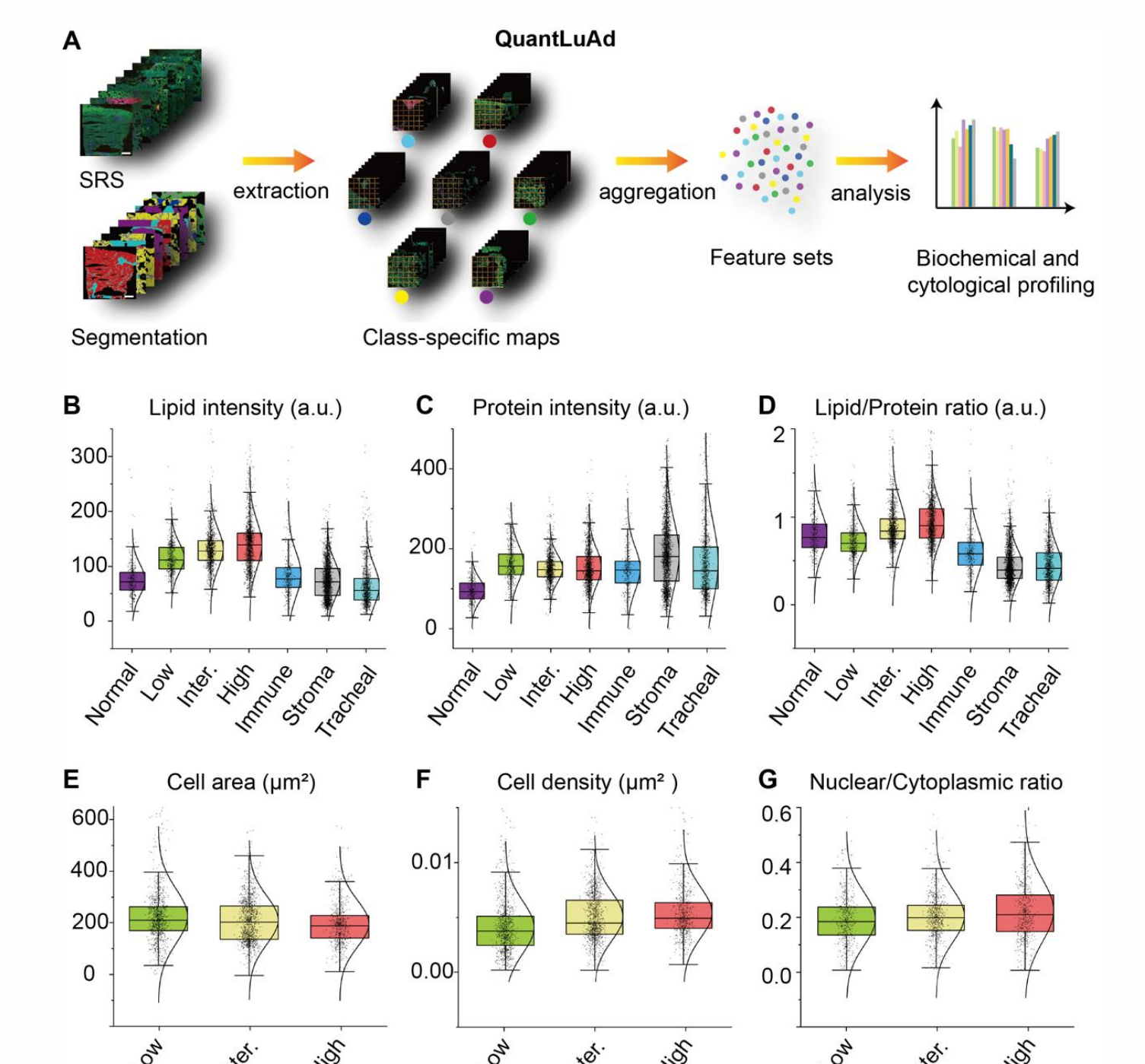


**Figure 4. QuantLuAd module for biochemical and cytological analysis based on segmentation results.** (A) Workflow of QuantLuAd, including segmentation-based image extraction, aggregation and statistical analysis. (B-D) Biochemical profiling including the intensity distributions of lipid, protein and lipid/protein ratio across the seven tissue subtypes. (E-G) Cytological profiling including cell size, cell density and nuclear/cytoplasmic ratio in low-, intermediate-, and high-grade tumor regions. a.u.: arbitrary units. Scale bars: 1000  $\mu$ m in (A).

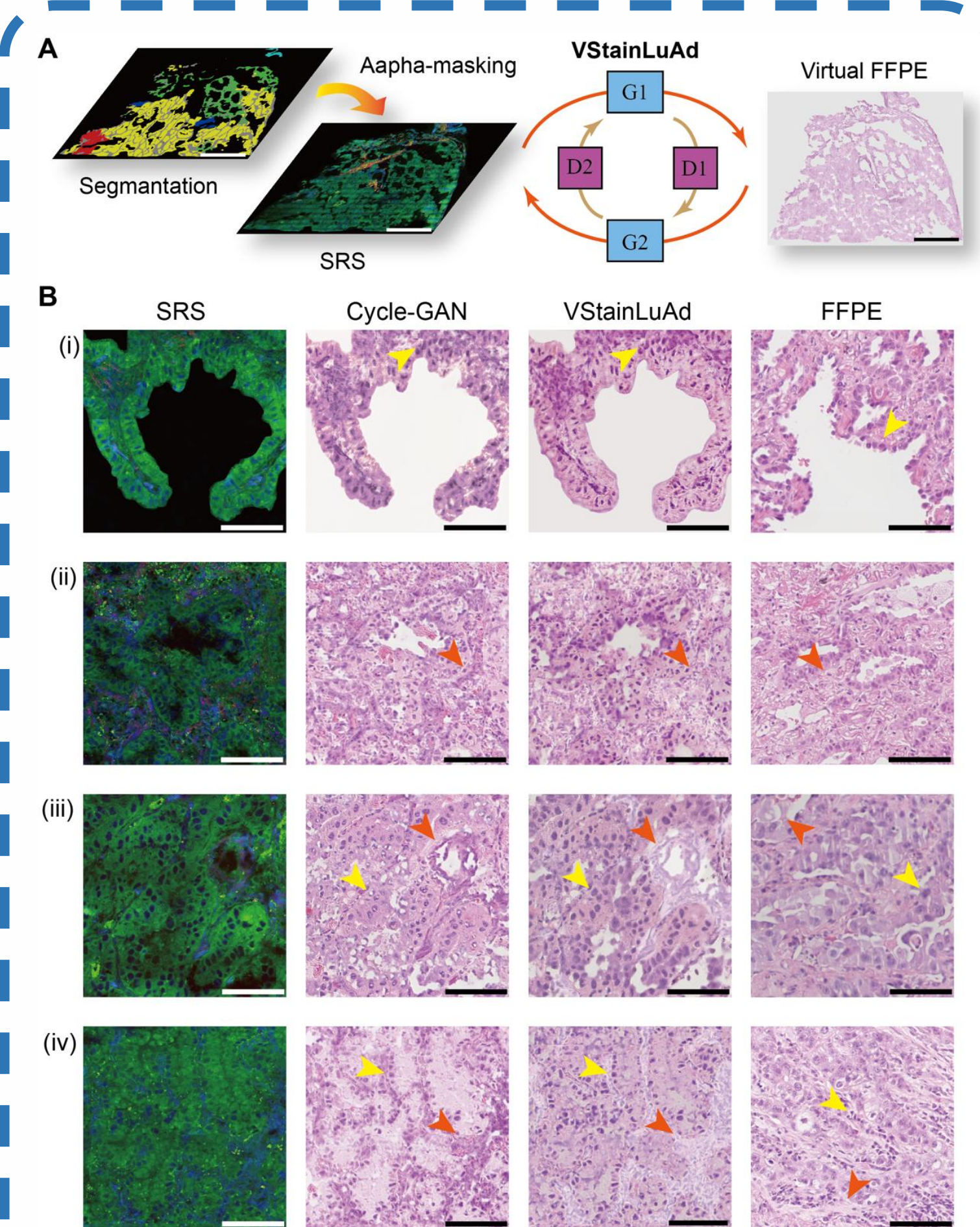


**Figure 5. Semantic-fused virtual staining with VStainLuAd module.** (A) Workflow of VStainLuAd framework incorporating segmentation maps into a CycleGAN architecture for virtual FFPE-style H&E staining. (B) Comparison of virtual staining results using conventional CycleGAN, VStainLuAd, and FFPE H&E stains (truth) across four representative lung tissue regions, showing improved nuclear-cytoplasmic contrast (yellow arrow) and enhanced structural fidelity in stromal (orange arrow). Scale bars: 1000  $\mu$ m in (A), 100  $\mu$ m in (B).

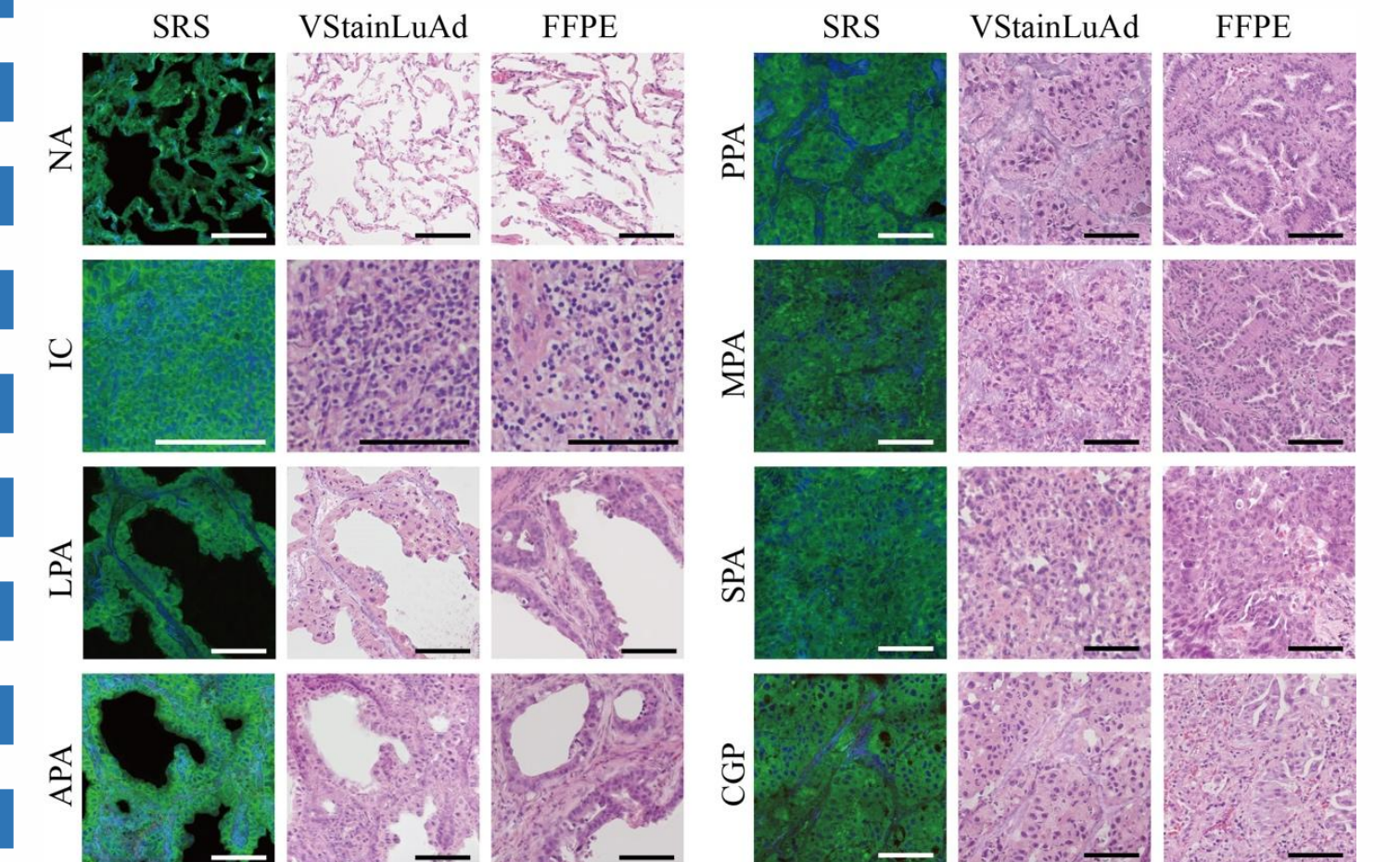


**Figure 6. Representative virtual staining results for eight subtypes of lung tissue.** NA: Normal alveoli; IC: immune cells; LPA: lepidic predominant adenocarcinoma; APA: acinar predominant adenocarcinoma; PPA: papillary predominant adenocarcinoma; MPA: micropapillary predominant adenocarcinoma; SPA: solid predominant adenocarcinoma; CPA: complex glandular patterns. Scale bars: 100  $\mu$ m.

## Conclusion

Collectively, we have systematically investigated the histologic imaging capability using SRS microscopy, and developed DeepLuAd as an integrated AI platform for semantic-guided tumor grading, quantification and virtual H&E staining. Our findings highlight the potential of DeepLuAd as a rapid, quantitative, and interpretable tool for digital histopathology of lung adenocarcinoma, paving the way for broader clinical translation of SRS imaging in cancer diagnosis and research.

Ma, L. et al. *Theranostics* 16, 2324-2341 (2026).  
<https://doi.org/10.7150/thno.125443> (current IF = 13.3)